沉积学报
ACTA SEDIMENTOLOGICA SINICA
ISSN 1000-0550
CN 62-1038/P

向上变浅序列的识别及沉积环境判识——以上扬子北缘寒武系洗象池组为例

唐佳全, 王瀚, 张耀云, 王斌, 邓豪爽, 侯明才

引用本文:
唐佳全, 王瀚, 张耀云, 等. 向上变浅序列的识别及沉积环境判识——以上扬子北缘寒武系洗象池组为例[J]. 沉积学报, 2026, 44(1): 87-105.
TANG JiaQuan, WANG Han, ZHANG YaoYun, et al. Recognition and Depositional Environment Interpretation of the Shallowing-Upward Sequence: A case study from the Cambrian Xixiangchi Formation in the northern margin of the Upper Yangtze[J]. *Acta Sedimentologica Sinica*, 2026, 44(1): 87-105.

引用格式：唐佳全，王瀚，张耀云，等.2026.向上变浅序列的识别及沉积环境判识——以上扬子北缘寒武系洗象池组为例[J].沉积学报，44(1): 87-105.
TANG JiaQuan, WANG Han, ZHANG YaoYun, et al. 2026. Recognition and Depositional Environment Interpretation of the Shallowing-Upward Sequence: A case study from the Cambrian Xixiangchi Formation in the northern margin of the Upper Yangtze[J]. Acta Sedimentologica Sinica, 44(1): 87-105.
DOI: 10.14027/j.issn.1000-0550.2024.046 CSTR: 32268.14/j.cjxb.62-1038.2024.046

向上变浅序列的识别及沉积环境判识
——以上扬子北缘寒武系洗象池组为例

唐佳全[1]，王瀚[1]，张耀云[2]，王斌[1]，邓豪爽[1]，侯明才[1]
1.油气藏地质及开发工程全国重点实验室(成都理工大学)，成都 610059
2.中国石油集团东方地球物理勘探有限责任公司西南物探研究院，成都 610093

摘 要 **【目的】**向上变浅序列在浅水碳酸盐环境中广泛发育，深时碳酸盐岩向上变浅序列的识别，对于分析浅水碳酸盐岩沉积环境演化具有独特优势。**【方法】**通过对上扬子北缘城口修齐镇上寒武统洗象池组进行详细的野外沉积学解剖和室内微相解析，识别碳酸盐岩向上变浅序列，分析其组合特征和纵向叠置关系，进而探讨上扬子地区晚寒武世沉积环境演化过程。**【结果】**在洗象池组中识别出MF0泥页岩、MF1泥粉晶灰岩、MF2亮晶砾屑灰岩、MF3亮晶砂屑灰岩、MF4泥质粉砂岩、MF5云质微晶灰岩、MF6砾屑白云岩、MF7亮晶砂屑白云岩、MF8砂质砾屑白云岩、MF9砂质砂屑白云岩、MF10砂质白云岩、MF11纹层状白云岩、MF12竹叶状砾屑白云岩、MF13具有溶蚀孔洞晶粒白云岩为主的14类沉积微相；根据微相组合关系，识别出C1-1、C1-2、C1-3、C1-4、C1-5、C1-6分米级向上变浅的潮下沉积序列、C2-1、C2-2、C2-3、C2-4、C2-5、C2-6分米级向上变浅的潮下—潮间沉积序列、C3-1、C3-2分米级向上变浅的潮间—潮上沉积序列，这些分米级向上变浅旋回构成3个次级海侵—海退沉积旋回，而3个次级旋回又从下至上构成洗象池组1个快速海侵—缓慢海退的向上变浅沉积旋回。**【结论】**基于识别向上变浅沉积序列并分析其组合特征、纵向叠置关系，认为上寒武统洗象池组受高频海平面变化影响明显，整体经历了早期快速海侵、晚期缓慢海退并发生多期次级海平面升降旋回，形成以混积潮坪亚相、云质潟湖亚相、台内颗粒滩亚相为典型沉积特征的局限碳酸盐岩台地沉积模式。同时，也进一步证实了晚寒武世发生了全球性的海平面下降事件。

关键词 上扬子北缘；洗象池组；碳酸盐岩微相；向上变浅序列；沉积环境判识

第一作者 唐佳全，男，1998年出生，硕士研究生，沉积地质学，E-mail: TangJiaQuan98@163.com
通信作者 侯明才，男，教授，E-mail: houmc@cdut.edu.cn

中图分类号：P534.41 **文献标志码**：A **文章编号**：1000-0550(2026)01-0087-19

0 引言

浅水碳酸盐岩环境中普遍发育向上变浅序列(谭秀成等，2014)。20世纪60年代，研究者发现在碳酸盐岩地层中常出现小尺度的向上变浅沉积单元(Laporte，1967；Coogan，1969)，之后逐渐将其归纳为浅滩化沉积序列(Wilson，1975)或向上变浅沉积序列(James，1978)。其成因目前还未定论，主要认为是由海平面升降、沉积作用、构造作用(Tucker and Wright，2015)、天文轨道力等多因素综合控制(Imbrie and Imbrie，1980；Goldhammer *et al.*，1987)。理想向上变浅沉积序列由环潮坪相、陆上暴露面或海泛面为界的潮下带多次重复沉积构成，并具有一系列明确的微相，包括浅潮下带、潮间带、潮上带和陆上暴露沉积作用特征(Flügel，2006)，不同微相组成的旋回叠置样式指示不同的沉积环境，如洛菲尔旋回指示潮坪环境(Fischer，1964)，Latemar旋回指示潮下陆棚环境(Goldhammer *et al.*，1990)。因此，深时碳酸盐岩向上变浅序列的识别，对于精准判识浅水碳酸盐岩沉积环境及演化特征具有独特优势。

收稿日期：2023-10-23；**修回日期**：2024-03-20；**录用日期**：2024-04-26；**网络出版日期**：2024-04-26
基金项目：国家自然科学基金项目(42102138)；自然资源部深时地理环境重建与应用重点实验室开放基金(DGERA20221103)

上扬子晚寒武世洗象池组为构造相对稳定的碳酸盐岩台地沉积，受全球海平面变化影响明显，分析其沉积环境特征对理解晚寒武世全球环境变化具有重要参考价值。前人对上扬子洗象池组沉积特征（石书缘等，2015；林怡等，2017；郭艳波等，2021）、沉积相类型（井攀等，2016b；刘鑫等，2018；张芮，2018）、层序地层（井攀，2017；白壮壮等，2021；曹庆超等，2021）与沉积环境（李伟等，2012；贾鹏等，2016；文华国等，2022）等方面开展了大量研究，但目前对洗象池组沉积旋回划分以及沉积模式还存在不同的认识。首先，不同学者在洗象池组分别识别出7个（陈洪德等，2002；梁乘鹏，2019）、5个（文华国等，2022）、4个（李伟等，2019；白壮壮等，2021；曹庆超等，2021）、3个（李文正等，2019；邓成昆等，2022；章学刚，2022）、2个（李茜等，2022）、1个（陈文等，2016；井攀，2017）海侵—海退沉积旋回。除此之外，部分学者认为洗象池组为局限台地沉积（胡朝阳，2015；井攀，2017；刘鑫等，2018；谷明峰等，2020；谢环羽等，2021；郭艳波等，2021；李璐萍等，2022；文华国等，2022）；另一部分学者则将洗象池组归纳为碳酸盐岩缓坡沉积（王瀚等，2019）。上扬子北缘晚寒武世洗象池组为一套连续的浅水碳酸盐岩沉积，发育典型向上变浅沉积序列，为利用高精度向上变浅序列分析晚寒武世沉积环境和演化特征提供了新的研究手段。

因此，本文选择上扬子台地北缘城口修齐镇洗象池组剖面为研究对象。通过野外沉积学特征解剖和室内碳酸盐岩微相解析，识别分米级—米级碳酸盐岩向上变浅序列，并基于向上变浅序列的组合和叠置关系进一步分析晚寒武世沉积环境演化、相对海平面变化特征，进而建立相应的沉积模式。该研究不仅详细刻画了扬子地区晚寒武世沉积环境演化特征，还对全球晚寒武世海平面变化提供了一定约束。

1 地质背景

研究区位于北大巴山逆冲推覆构造带前缘、城口断裂带南侧的厚坪一带（图1），属于上扬子台地北缘（齐哲等，2022）。上扬子地区前寒武时期发生晋宁运动与澄江运动，形成了复杂的盆地基底，并在其上沉积震旦系盖层（谢环羽等，2021）。震旦纪末期—早寒武纪的桐湾运动致使四川盆地全面抬升剥蚀，导致震旦系与寒武系呈假整合接触（黄福喜等，2011）；中寒武世—早奥陶世发生局部构造运动，米仓山地区抬升出露水面遭受剥蚀，导致该区域部分地层发生缺失（夏康杰，2020）；志留纪末期的加里东运动加剧了区域性剥蚀，形成了东低西高的古地理格局；二叠纪发生峨眉地裂运动影响了四川盆地构造沉积格局，川北地区形成坳拉槽群（罗志立，2012）；晚三叠世至早白垩世，由于板块运动活跃，盆地内部发生强烈的造山运动，龙门山—米仓山—大巴山与四川盆地周缘在此时隆起，盆地的雏形就此形成（黄丹，2012）；晚白垩世至第四纪，四川盆地整体隆升并伴随剥蚀，盆地边缘变形强烈，内部变形较弱（潘安，2019）。

晚寒武世时期，上扬子为一套受陆源碎屑影响的稳定碳酸盐岩沉积（黄福喜等，2011）。研究区中—晚寒武世地层发育齐全，实测剖面自下而上划分为中寒武统覃家庙组、上寒武统洗象池组以及下奥陶统杨家坝组。洗象池组与下伏覃家庙组整合接触，与上覆奥陶统杨家坝组呈不整合接触关系。前人研究表明，覃家庙组处于寒武系第二次海退的晚期阶段，主要发育一套以云质泥岩、粉砂质泥岩为主的混积潮坪沉积（张芮，2018）。随后在中—晚寒武世洗象池组早期发生第三次海侵，随着海平面快速上升，陆源碎屑供给减少，主要发育以灰岩、白云岩为主的碳酸盐岩台地沉积；洗象池组晚期处于第三次海退时期，以陆源碎屑含量较高的混积潮坪沉积为主，在洗象池组顶部发育不整合面与古风化壳（图2a）（张满郎等，2010；王瀚等，2019）。

2 主要微相类型及解释

根据野外露头精细解剖和室内岩石薄片鉴定结果，参考Flügel（2010）沉积微相划分方案，确定城口修齐剖面洗象组主要发育14种微相类型（表1），按照微相沉积环境分为潮下带沉积微相MF0~MF10；潮间带沉积微相MF11~MF12；潮上带沉积微相MF13；下面将具体介绍主要沉积微相的特征及分析解释结果。

泥页岩MF0：主要发育于各沉积旋回底部，野外露头呈黑色—深黑色薄层状产出，厚约2~20 cm不等，发育水平层理。该微相认为是悬浮在水中的黏土物质在较平静水动力条件下缓慢沉降形成，水平层理为细粒沉积物在静水环境中发生垂向加积作用沉淀而成。推测MF0是最大海泛面沉积，位于开阔

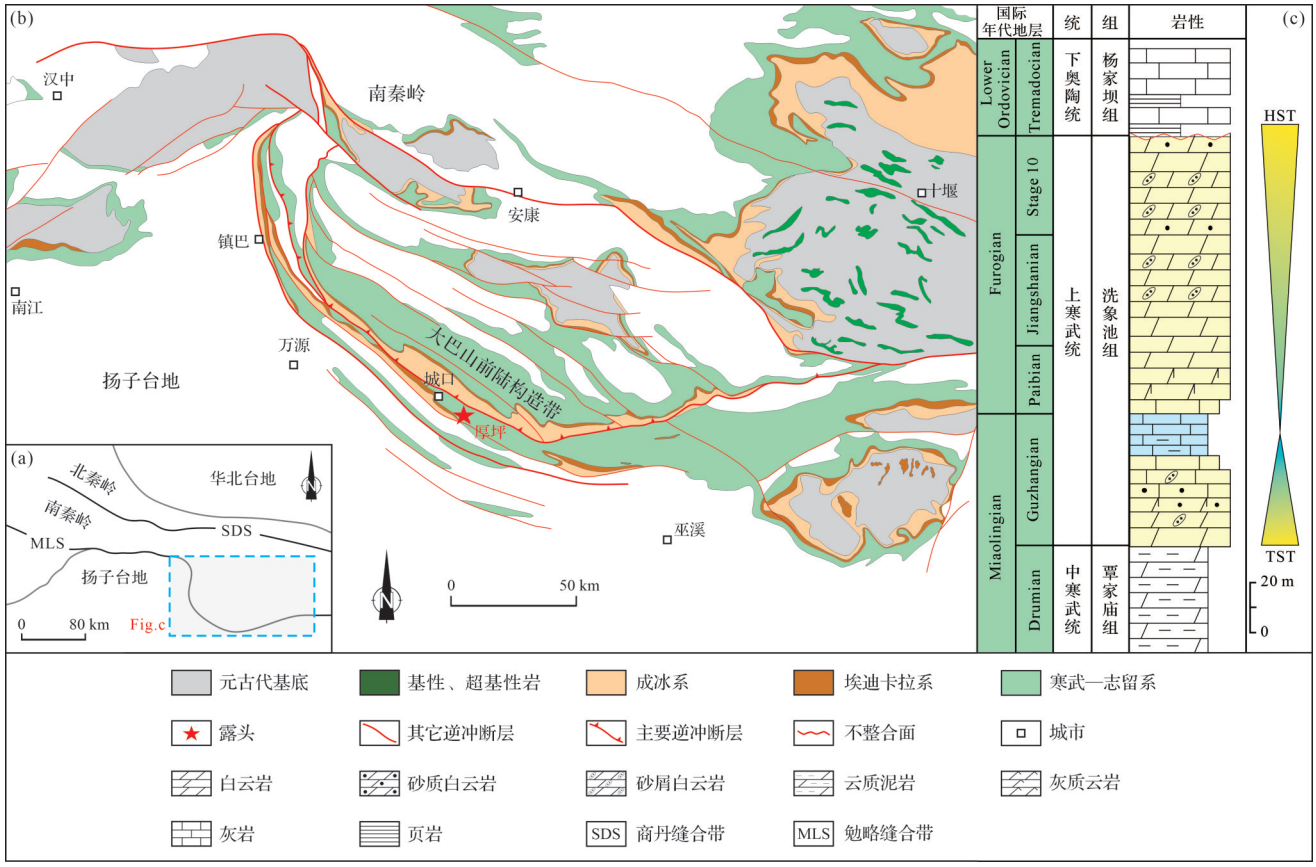

图1　上扬子地台北缘区域地质简图及上寒武统洗象池组综合柱状图(Wang *et al.*, 2022)

(a)上扬子地台北缘主要构造单元简化地质图;(b)上扬子地台震旦纪—寒武纪地层简图;(c)上扬子地台北缘上寒武统洗象池组综合柱状图

Fig.1　Geological map of the northern margin of the Upper Yangtze Platform and comprehensive histogram of the upper Cambrian Xixiangchi Formation (Wang *et al.*, 2022)

(a) simplified geological map of the main tectonic units from the northern margin of the Upper Yangtze Platform; (b) Sinian-Cambrian stratigraphic map of the Upper Yangtze Platform; (c) comprehensive histogram of the upper Cambrian Xixiangchi Formation in the northern margin of the Upper Yangtze Platform

或局限的潮下带深水低能环境。

泥粉晶灰岩MF1:野外露头呈中—深灰色薄—中层状产出,局部发育水平层理;镜下方解石呈暗色、均质,以泥粉晶为主,晶粒小于4 μm,自形程度较差,呈镶嵌状接触,被茜红素染色,部分薄片可见少量泥晶方解石重结晶形成微亮晶方解石。镜下可见泥质纹层,具有水平层理,认为其形成于开阔潮下带深水低能环境。

亮晶砾屑灰岩MF2:主要发育于洗象池组下段,野外露头呈中灰色中层状产出。颗粒以砾屑为主,含量约为85%,以亮晶胶结为主,胶结物含量约为15%,砾屑呈椭圆状,分选中等,磨圆呈次圆状,杂乱状分布,无定向排列;部分颗粒周缘边界模糊,有磨蚀、破损现象,颗粒内部泥晶方解石重结晶为细晶方解石,具残余砾屑结构。根据其颗粒粒度、形态与分布性特征,推测是风暴、波浪及潮汐作用对半固结沉积物不断冲刷、侵蚀改造,并经历短距离搬运作用形成,其沉积环境为开阔潮下带强振荡水体环境。

亮晶砂屑灰岩MF3:主要发育于洗象池组下段,野外露头呈浅—中灰色中层状产出。镜下颗粒以砂屑为主,砂屑含量为80%,呈亮晶胶结,胶结物含量约为20%;颗粒磨圆呈次棱角状—次圆状,分选差—中等(图3a)。其形成是较强水动力对原有碳酸盐质灰泥打碎、淘洗、筛选形成砂屑颗粒,并且海水发生化学沉淀形成亮晶胶结。推测该微相沉积环境为开阔潮下带中等振荡水体环境。

泥质粉砂岩MF4:主要发育于洗象池组中上部,野外露头呈灰黑色、灰绿色薄层状产出(图2b)。其形成是由于海平面下降,沉积环境由开阔转为局限,水体流动减少,水动力减弱,漂浮于海水中的黏土物质与粉砂在静水环境中沉降到海底固结成岩。推测该微相沉积环境为局限潮下带深水低能环境。

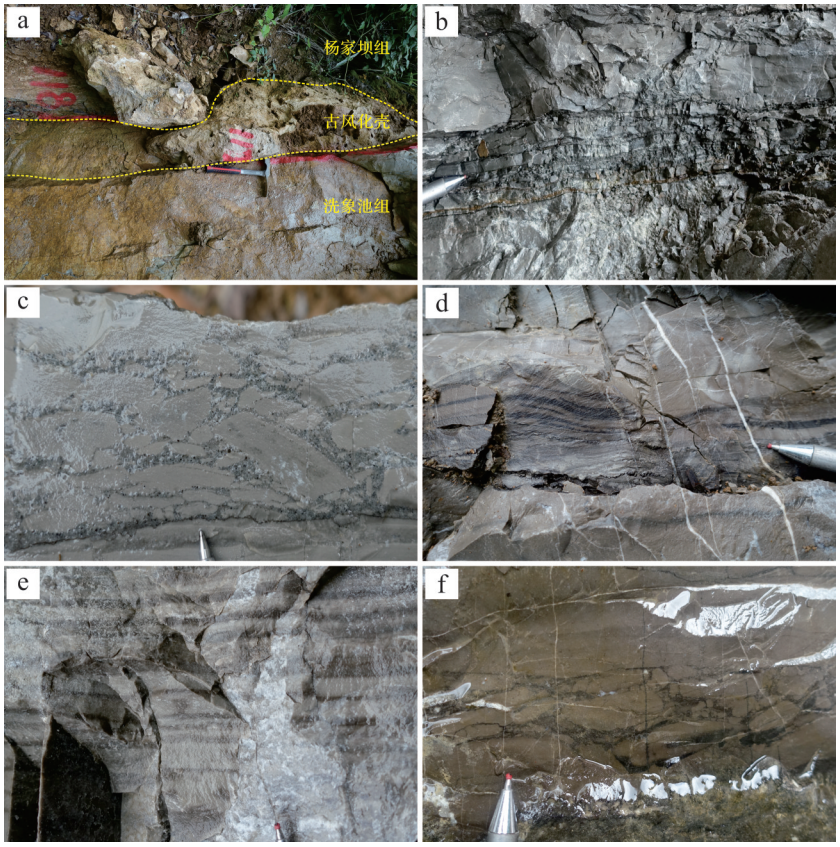

图2 川北城口修齐剖面上寒武统洗象池组野外沉积特征

(a)洗象池组顶部古风化壳,古风化壳凹凸不平,发育溶洞,由泥质充填;(b)深灰色薄层状泥质粉砂岩;(c)风暴砾屑段,砾屑形态为长条状、椭圆状,呈倒八字形分布,颗粒间充填大量陆源碎屑颗粒;(d)丘状交错层理,起伏较为明显,其下部发育底冲刷构造;(e)纹层状白云岩,亮层与暗层界限分明,交替沉积;(f)干裂收缩竹叶状砾屑,砾屑形态为长条状、椭圆状,呈叠瓦状分布;砾屑间为暴露成因的泥裂,陆源碎屑、泥质充填

Fig.2 Field sedimentary characteristics of the upper Cambrian Xixiangchi Formation in the Xiuqi section of Chengkou, northern Sichuan Basin

(a) the ancient weathering crust at the top of the Xixiangchi Formation, the ancient weathering crust is uneven, the development of karst caves, filled by mud; (b) dark gray thin bedded argillaceous siltstone; (c) storm debris section, the debris is in the shape of long strip and oval, showing an inverted eight-shaped distribution, and a large number of terrigenous debris particles are filled between the particles; (d) the hummocky cross-bedding has clear undulation, and the bottom erosion structure is developed in the lower part; (e) laminated dolomite, bright layer and dark layer boundary with clear alternating deposition; (f) dry cracking shrinkage bamboo leaf-like gravel, gravel shape is long strips, oval, imbricate distribution. exposed mud cracks, terrigenous debris, and muddy fillings are seen between the gravel

云质微晶灰岩MF5:野外露头呈中灰色中层状产出,含有少量黑色黄铁矿。镜下方解石以粉晶为主,含量约为55%,自形程度较差,呈镶嵌式接触;白云石含量约为45%,以微晶为主,为方解石白云石化产物,部分晶粒白云石化不彻底,常呈他形镶嵌于粉晶方解石中(图3b)。该岩性为灰岩与白云岩的过渡岩性,为微晶结构,认为其发育于局限潮下带深水低能环境。

砾屑白云岩MF6:野外露头呈中灰色中层状砾屑层产出,砾屑形态为长条状、椭圆状,呈菊花状、叠瓦状顺层延伸(图2c),部分层位砾屑呈正粒序分布;底部发育底冲刷构造,上部可见丘状交错层理(图2d)。镜下砾屑颗粒含量约为80%,颗粒形态为长条状、撕裂状,分选差—中等,磨圆呈次圆状、次棱角状,杂乱状分布;可见少量分选中等、磨圆呈次圆状—次棱角状的陆源石英分布于砾屑颗粒间,含量约为5%(图3c)。砾屑菊花状、叠瓦状或撕裂状的排列方式反映了风暴涡流作用(王瀚等,2019),而两种不同成分的砾屑颗粒指示风暴流搬运造成不同成分砾屑的混合作用;底冲刷构造是由风暴流对沉积物底面进行侵蚀、改造形成的再沉积充填沉积构造;丘状交错层理为风暴远端振荡流、摆动流作用的产物(金鑫等,2021);粒序层理为风暴作用衰退期,风暴流搬运的砾屑逐渐减少进而在侵蚀面上伏形成正粒序(王牧源等,2024);撕裂的内碎屑与石英颗粒可能为风暴回流带来沉降于砾屑颗粒间。推测该微相形

表1　重庆城口修齐剖面上寒武统洗象池组微相分类表

Table 1　Microfacies classification of the upper Cambrian Xixiangchi Formation in the Xiuqi section of Chengkou, Chongqing

城口修齐剖面洗象池组微相名称	发育层位	标准微相(SMF)(Flügel,2010)	沉积环境
MF0泥页岩	洗象池组下部	未划分	开阔或局限潮下带 深水低能环境
MF1泥粉晶灰岩	洗象池组下部	SMF8	开阔潮下带 深水低能环境
MF2亮晶砾屑灰岩	洗象池组下部	SMF10	开阔潮下带 强振荡水体环境
MF3亮晶砂屑灰岩	洗象池组下部	SMF11	开阔潮下带 中等振荡水体环境
MF4泥质粉砂岩	洗象池组中、上部	未划分	局限潮下带 深水低能环境
MF5云质微晶灰岩	洗象池组中、下部	未划分	局限潮下带 深水低能环境
MF6砾屑白云岩	洗象池组全段	SMF12	局限潮下带 强振荡水体环境
MF7亮晶砂屑白云岩	洗象池组全段	SMF16	局限潮下带 中等振荡水体环境
MF8砂质砾屑白云岩	洗象池组全段	SMF17	局限潮下带 中等振荡水体环境
MF9砂质砂屑白云岩	洗象池组全段	SMF18	局限潮下带 中等振荡水体环境
MF10砂质白云岩	洗象池组全段	未划分	局限潮下—潮间带 中等振荡水体环境
MF11纹层状白云岩	洗象池组中—上部	SMF19	潮间带 局限暴露环境
MF12竹叶状砾屑白云岩	洗象池组中—上部	SMF24	潮间带 局限暴露环境
MF13具溶蚀孔洞晶粒白云岩	洗象池组上部	SMF21	潮上带 蒸发、暴露环境

成主要受风暴作用的影响,其沉积环境为正常浪基面与风暴浪基面之间,为局限潮下带强振荡水体环境。

亮晶砂屑白云岩MF7:野外露头呈浅—中灰色中层状产出。镜下砂屑颗粒含量约80%,少量颗粒呈点、线接触,大部分颗粒呈亮晶胶结,分选较好—中等,磨圆呈次圆状、次棱角状;颗粒边缘发育暗色泥晶包壳,内部为泥晶白云石;亮晶胶结,胶结物含量约为20%(图3d)。根据砂屑颗粒类型,认为是在强波浪和潮汐作用下对原有的沉积物进行了冲刷、淘洗、筛选,海水发生化学沉淀形成亮晶胶结,固结成岩而成。推测其发育于局限潮下带中等振荡水体环境。

砂质砾屑白云岩MF8:野外露头呈中灰色中层状产出。镜下砾屑含量约为75%,呈长条状、椭圆状,分选差,磨圆呈次圆状,整体杂乱状分布,砾屑成分为泥晶白云石,为原有白云石泥沉积物被强水动力破碎形成;陆源石英含量约25%,分选中等,磨圆呈次圆状—次棱角状,分布于砾屑颗粒间,部分石英颗粒与砾屑颗粒镶嵌式接触(图3e)。其形成主要受波浪、潮汐作用控制,涨潮时,波浪将原有沉积物打碎、淘洗形成砾屑,古陆被侵蚀而提供大量陆源碎屑供给;退潮时,波浪沿岸流将陆源碎屑带入海洋与白云岩砾屑混合沉积。推测该微相发育于水体较浅、离岸较近、环境相对闭塞的局限潮下带中等振荡水体环境。

砂质砂屑白云岩MF9:野外露头呈中灰色中层状产出,颗粒以砂屑为主,含有细—中粒黑色燧石。镜下砂屑颗粒含量约为75%,由泥晶基质构成,磨圆呈次棱角状、次圆状,分选中等,部分颗粒发生重结晶作用,呈残余砂屑结构;陆源石英含量约25%,以细粒、中粒为主,分选差,磨圆呈次棱角状、次圆状,

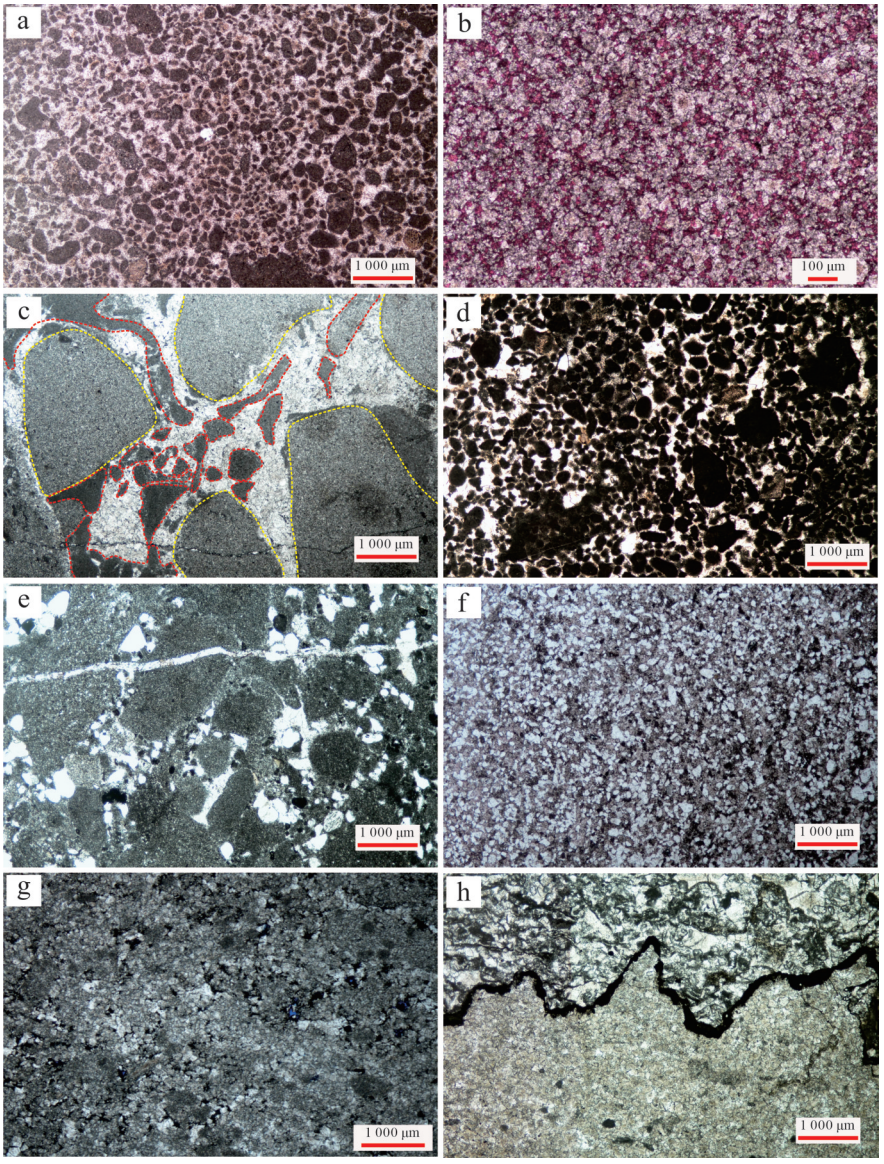

图3 川北城口修齐剖面上寒武统洗象池组镜下沉积特征

(a)MF3亮晶砂屑灰岩,砂屑分选中等,磨圆呈次圆状、次棱角状,部分砂屑发生重结晶,亮晶胶结,单偏光;(b)MF5云质微晶灰岩,泥晶方解石发生白云石化形成粉晶白云石呈网状分布,单偏光;(c)MF6砾屑白云岩,椭圆状、撕裂状、断裂状砾屑无定向排列呈杂乱状分布;砾屑颗粒按成分分为两种,一种为粉晶白云石构成(黄色虚线)、另一种为泥晶白云石构成(红色虚线),单偏光;(d)MF7亮晶砂屑白云岩,砂屑颗粒分选中等,磨圆呈次圆状—次棱角状,亮晶胶结,单偏光;(e)MF8砂质砾屑白云岩,砾屑颗粒呈椭圆状、长条状,分选差—中等,磨圆呈次圆状,由泥晶白云石构成;砾屑颗粒间充填中—粗粒陆源石英,单偏光;(f)MF10砂质白云岩,石英颗粒以细砂为主,呈次棱角状杂乱分布于粉晶白云石间;单偏光;(g)MF13具溶蚀孔洞晶粒白云岩,溶蚀现象明显,发育较多晶间孔、缝,沥青半充填,少量孔隙未被充填呈蓝色,铸体薄片,单偏光;(h)MF13具溶蚀孔洞晶粒白云岩,发生溶蚀垮塌,砾屑白云岩与细晶白云岩杂乱堆积,形成缝合线构造,单偏光

Fig.3 Microscopic sedimentary characteristics of the upper Cambrian Xixiangchi Formation in the Xiuqi section of Chengkou, northern Sichuan Basin

(a) MF3 bright crystal calcarenite, with medium sand sorting, sub-circular and sub-angular shape, sand debris recrystallization phenomenon, bright crystal cementation, single polarization, plane polarized light (PPL); (b) MF5 dolomitic microcrystalline limestone and micritic calcite forms powder crystal dolomite into network distribution, PPL; (c) MF6 gravel dolomite, oval, torn, fractured gravel without directional arrangement is disorderly distribution; the gravel particles are divided into two types based on the composition, one is composed of powder crystal dolomite (yellow dotted line), and the other is composed of mud crystal dolomite (red dotted line), PPL; (d) MF7 brilliant crystalline sandy dolomite, medium sorting of sand-debris particles, sub-circular and sub-angular shape, bright crystal cementation, PPL; (e) MF8 sandy gravel dolomite, gravel particles are oval, long strip, poor-medium sorting, grinding round is sub-circular, composed of micritic dolomite; the gravel particles are filled with medium-coarse terrestrial quartz, PPL ; (f) MF10 sandy dolomite, quartz particles are mainly fine sand, sub-angular disorderly distributed between powder crystal dolomite, PPL; (g) MF13 grain dolomite with dissolved pores and holes, the dissolution phenomenon is obvious, the development of more intergranular pores, cracks, asphalt semi-filled, a small amount of pores are not filled in blue, casting thin section, PPL; (h) MF13 grain dolomite with corrosion holes is corroded and collapsed, and the gravel dolomite and fine-grained dolomite are disorderly stacked to form a suture structure, PPL

充填于白云石砂屑之间。推测其是海侵过程中白云石泥沉积物被海水破碎形成砂屑,而后沿岸流分选出少量的陆源石英分布于砂屑颗粒之间,形成混合沉积物,认为其发育于局限潮下带中等振荡水体环境。

砂质白云岩MF10:野外露头呈中灰色中层状或条带状产出,部分层位陆源石英呈正粒序分布。镜下白云石含量约为60%,以细晶为主;陆源石英含量约为40%,以细—中粒为主,分选中等—较差,磨圆呈次圆状—次棱角状(图3f)。根据石英颗粒的产状,认为是在海平面上升过程中,海岸受到风暴、波浪的冲刷、侵蚀作用,进而提供大量陆源碎屑,且未经过远距离搬运与白云石泥混合沉积;正粒序层理是由于风暴作用减弱,流体能量降低、流速减缓,陆源碎屑颗粒发生重力分异作用快速沉降形成。推测该微相发育于正常浪基面与平均低潮线之间,沉积环境为局限潮下带中等振荡水体环境。

纹层状白云岩MF11:露头上表现为灰白色薄层状云岩与暗色薄层状云岩互层,两者纵向上呈韵律状相间沉积形成细密平直纹层(图2e)。镜下亮层与暗层界限明显,亮层以亮晶白云石为主,暗层以泥—粉晶白云石为主;发育鸟眼孔构造,被粗晶白云石充填。细密平直纹层为沉积条件短期变化形成,指示了间歇性变化的低能水动力环境:暗色纹层为潮落时在安静水体中沉积;亮层为涨潮时淹没、冲刷原有白云石泥,海水化学沉降亮晶白云石形成。鸟眼孔构造指示暴露环境。推测该微相沉积环境为潮间带局限暴露环境。

竹叶状砾屑白云岩MF12:野外露头呈浅灰色薄层状产出,砾屑颗粒形态为竹叶状、长条状,呈叠瓦状分布,砾屑间充填渗流粉砂,发育泥裂构造(图2f)。镜下砾屑呈竹叶状、长条状,砾屑内部为泥—粉晶白云石,分选中差,磨圆呈次棱角状—次圆状;颗粒间存在渗流粉砂,石英颗粒分选差,磨圆呈次棱角状。其形成过程为原有沉积物在暴露于水面后,发生脱水作用,干裂收缩形成泥裂以及长条状、竹叶状砾屑原地沉积;当海平面上升,水流带来的碎屑物质沿着裂隙充填。推测该微相形成于潮间局限暴露环境。

具溶蚀孔洞晶粒白云岩MF13:野外露头浅灰色中—厚层状产出,岩溶现象丰富,发育大量溶蚀孔、洞和溶蚀缝,部分孔、缝被泥质、方解石充填,另一部分被有机质充填,可见大片浸染状沥青;部分层位发育块状岩溶垮塌角砾。镜下以细晶、中晶白云石为主,含量约为95%,泥质、有机质、石英总量约为5%;常见溶孔、溶洞与方解石脉以及缝合线伴生发育,部分孔、洞、缝被沥青充填(图3g,h)。其形成过程认为是局限环境中形成的泥晶白云岩,由于海平面下降,蒸发作用增强,盐度以及碱度升高,发生重结晶形成较粗晶粒白云岩;随着水体不断变浅,沉积物暴露于水面上,遭受风化淋滤作用造成大量溶蚀;岩溶形成的大孔洞在上覆岩层的压力作用下发生塌陷形成块状岩溶角砾。推测该微相发育环境局限的潮上带蒸发、暴露环境。

3　典型向上变浅沉积序列识别与沉积环境判识

研究发现城口地区洗象池组共发育14种沉积微相,这些微相在纵向上相互组合并叠置沉积形成若干个厘米、分米、米级向上变浅沉积旋回,揭示了碳酸盐岩台地发生高频振荡海平面升降变化。城口剖面洗象池组以局限台地沉积为主,根据微相的组成和排列,确定3种沉积序列、14种岩相组合类型。旋回类型Ⅰ(C1):潮下旋回(图4a,b);旋回类型Ⅱ(C2)潮下—潮间旋回(图4c,d);旋回类型Ⅲ(C3):潮缘旋回。

旋回类型Ⅰ(C1)潮下旋回,主要发育于洗象池组中下部,通过对沉积结构、构造、微相的分析,确定了6种亚类:C1-1发育于洗象池组下部,表现为MF1→MF3的沉积序列叠置沉积,旋回下部为中灰色薄层状泥粉晶灰岩,旋回上部为浅灰色中层状亮晶砂屑灰岩,反映了开阔潮下带深水低能水体环境—开阔潮下带中振荡水体环境的演化序列。C1-2发育于洗象池组下部,表现为MF5→MF7的沉积序列叠置沉积,旋回下部为中灰色薄—中层状云质微晶灰岩,上部为浅灰色中层状亮晶砂屑白云岩(图5),反映了局限潮下带深水低能环境—潮下带中等振荡水体环境的演化序列。C1-3发育于洗象池组下部,表现为MF0→MF10的沉积序列叠置沉积,旋回底部为厘米级暗色泥页岩,泥岩顶部发育底冲刷构造,上覆砂质白云岩,可见陆源碎屑呈正粒序分布,推测是风暴事件沉积,风暴流对原有泥质沉积冲刷、侵蚀形成底冲刷面,其携带的大量沿岸陆源碎屑在冲刷面上沉积,随着风暴能量减弱,陆源碎屑由于重力分异快

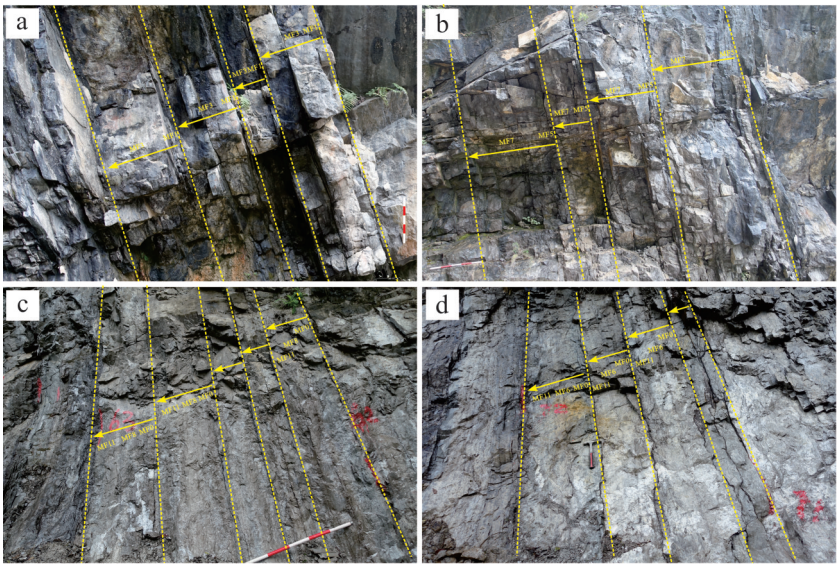

图4 川北城口修齐剖面上寒武统洗象池组典型向上变浅序列宏观照片

(a)潮下旋回,旋回下部为中灰色薄层状粉晶灰岩,上部为浅灰色中层状亮晶砂屑灰岩;(b)潮下旋回,旋回下部为中灰色薄层状云质微晶灰岩,旋回上部为浅灰色中层状亮晶砂屑白云岩;(c)潮下—潮间旋回,旋回底部为厘米级暗色泥页岩,下部为薄层状粉晶白云岩,中部为深灰色中层状砂质砾屑白云岩,上部为纹层状白云岩;(d)潮下—潮间旋回,旋回下部为厘米级暗色泥页岩,中部为中—深灰色中层状砾屑白云岩,上部为纹层状白云岩夹砂质条带

Fig.4 Macroscopic view of typical shallowing-upward sequence from the upper Cambrian Xixiangchi Formation in the Xiuqi section of Chengkou, northern Sichuan Basin

(a) subtidal cycle, the lower part of the cycle is medium-gray thin-bedded siltstone limestone, and the upper part is light-gray medium-bedded bright crystalline sandy limestone; (b) subtidal cycle, the lower part of the cycle is medium gray thin layer of dolomitic microcrystalline limestone, and the upper part of the cycle is light gray medium layered brilliant crystalline sandy dolomite; (c) subtidal-intertidal cycle, the bottom of the cycle is centimeter-level dark shale, the lower part is thin-layer powder crystal dolomite, the middle part is dark gray medium layered sandy gravel dolomite, and the upper part is lamellar dolomite; (d) subtidal-intertidal cycle, the lower part of the cycle is centimeter-level dark mud shale, the middle part is medium-dark gray medium layered gravel dolomite, and the upper part is layered dolomite with sandy strip

速沉降形成正粒序,反映了局限潮下带深水低能环境遭受风暴影响。C1-4发育于洗象池组中下部,表现为MF4→MF10的沉积序列叠置沉积,旋回下部发育约10 cm的暗色泥质粉砂岩,旋回上部为中层状微晶白云岩与砂质白云岩交替沉积,反映了局限潮下带深水低能水体环境—局限潮下带中等振荡水体环境的演化序列,受周期性海平面升降影响形成弱的间断式混积沉积。C1-5发育于洗象池组中下部,表现为MF6→MF10的沉积序列叠置沉积,底部发育明显的底冲刷面,旋回下部为菊花状、倒八状分布的砾屑段,砾屑颗粒间充填陆源石英,上部为砂质白云岩,呈正粒序分布。推测为风暴事件沉积,在风暴高峰期,风暴流卷入大量沿岸陆源碎屑物质并不断冲刷、拍打、簸选原有沉积物,形成杂乱状分布的砂质砾屑段,当风暴作用减弱,携带的陆源石英由于重力分异作用快速沉淀呈正粒序分布,反映了潮下带水体环境遭受风暴影响。C1-6发育于洗象池组上部,表现为MF4→MF8→MF10的沉积序列叠置沉积,旋回下部为3 cm泥质粉砂岩,中部为砂质砾屑白云岩,砾屑呈叠瓦状分布,上部为微晶白云岩与砂质白云岩交替沉积,其形成过程受周期性波动的波浪、潮汐控制,形成弱的原地式混积与间断式混积沉积,反映了局限潮下带深水低能环境—潮下带中等振荡水体环境的演化序列。

旋回类型Ⅱ(C2)潮下—潮间旋回,在洗象池组上中下段均发育此类沉积序列,通过对沉积结构、构造、微相的分析,确定了6种亚类:C2-1发育于洗象池组下部,表现为MF0→MF10→MF12的沉积序列叠置沉积,旋回底部为约5 cm暗色泥岩,旋回下部发育轻微冲刷底面构造,向上为浅灰色中层状微晶白云岩夹砂质条带,上部为竹叶状砾屑顺层分布,发育泥裂,裂缝间充填陆源石英颗粒,反映了局限潮下带深水低能环境—局限潮下带中等振荡水体环境—潮间带局限暴露环境的演化序列。C2-2发育于洗象池组下部,表现为MF0→MF6→MF10→MF12的沉积序列叠置沉积,旋回底部发育约5 cm暗色泥岩,其上部可见底冲刷构造与丘状交错层理,旋回下部发育砾屑段,砾屑颗粒形态为长条状,呈正粒序分布,旋回上

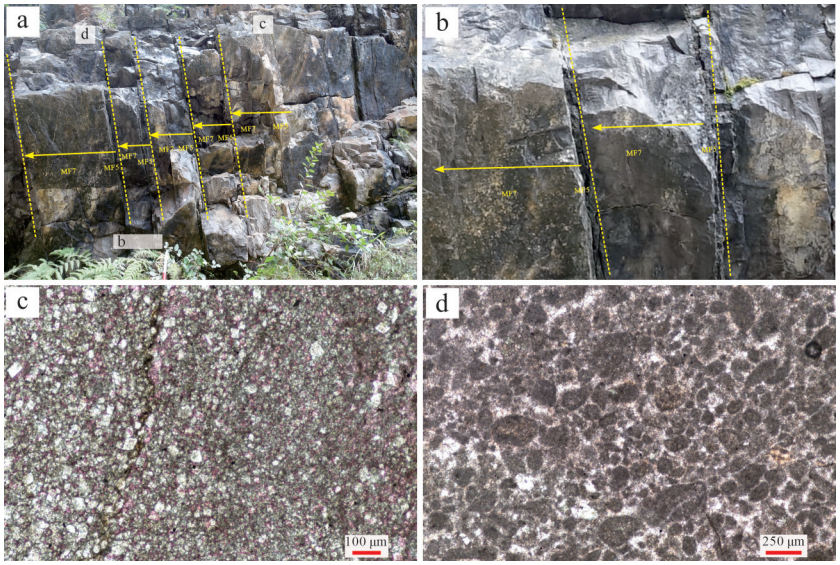

图5　川北城口修齐剖面上寒武统洗象池组潮下旋回C1-2宏—微观特征

(a)潮下沉积旋回宏观照,发育多个向上变浅沉积旋回;(b)旋回局部放大照,旋回下部为薄层状中灰色中层状云质微晶灰岩,旋回上部为中层状亮晶砂屑白云岩;(c)YMQ-40-2B,云质微晶灰岩,泥晶灰岩发生差异白云岩化,晶粒以泥、粉晶为主,单偏光;(d)YMQ-41-2B,亮晶砂屑白云岩,砂屑颗粒分选中等,磨圆呈次圆状,亮晶胶结,单偏光

Fig.5　Macro-micro characteristics of subtidal cycle C1-2 of the upper Cambrian Xixiangchi Formation in the Xiuqi section, Chengkou, northern Sichuan Basin

(a) macroscopically, the subtidal sedimentary cycle develops several upward shallowing sedimentary cycles; (b) the local amplification of the cycle shows that the lower part of the cycle is thin-bedded medium-gray medium-bedded dolomitic microcrystalline limestone, and the upper part of the cycle is medium-bedded brilliant crystalline sandy dolomite; (c) YMQ-40-2B, Dolomitic microcrystalline limestone, micritic limestone have different dolomitization, and the grains are mainly mud and powder crystals, PPL; (d) YMQ-41-2B, Brilliant crystalline sandy dolomite, sand particles are moderately sorted and rounded nearly sub-round, bright crystal cementation, PPL

部发育砂质白云岩,陆源碎屑呈正粒序分布,可见丘状交错层理发育,旋回顶部发育由泥裂形成的呈叠瓦状分布的竹叶状砾屑段,认为此序列受到风暴作用的控制,风暴回流搬运分选、磨圆较好的砾屑颗粒与碎屑颗粒,由于搬运距离的增加,回流的能量降低,砾屑颗粒与陆源碎屑呈正粒序分布沉积,随着水体深度变浅,其上发育暴露成因的竹叶状砾屑白云岩,反映了潮下带深水低能环境—潮下带强振荡水体环境—潮下带中等振荡水体环境—潮间带局限暴露环境的演化序列。C2-3发育于洗象池组中部,表现为MF0→MF8→MF11的沉积序列重复沉积,旋回底部约5 cm暗色泥页岩,下部为薄层状粉晶白云岩,中部为深灰色中层状砂质砾屑白云岩,上部为纹层状白云岩,反映了潮下带深水低能环境—潮下带中等振荡环境—潮间带局限暴露环境的演化序列。C2-4发育于洗象池组中部,表现为MF0→MF10→MF11的沉积序列重复沉积,旋回下部约5 cm暗色泥页岩,中部为砂质白云岩,呈层状分布,上部为纹层状白云岩(图6),反映了潮下带深水低能环境—潮下带中等振荡水体环境—潮间带局限暴露环境的演化序列。C2-5发育于洗象池组中上部,表现为MF0→MF11→MF12,旋回底部发育约3 cm暗色泥页岩,下部发育深灰色薄—中层状粉晶白云岩,中部发育纹层状白云岩,上部发育干裂收缩状竹叶状砾屑白云岩,反映了潮下带深水低能环境—潮间带局限暴露环境的演化序列。C2-6发育于洗象池组上部,表现为MF4→MF6→MF11,旋回下部为3 cm暗色泥质粉砂岩,中部为中—深灰色中层状砾屑白云岩,上部为纹层状白云岩夹砂质条带,反映了潮下带深水低能环境—潮下带强振荡水体环境—潮间带局限暴露环境的演化序列。

旋回类型Ⅲ(C3)潮缘旋回,潮间—潮上沉积序列,主要发育于洗象池组中上部,通过对沉积结构、构造、微相的分析,确定了2种亚类:C3-1发育于洗象池组上部,表现为MF12→MF14的沉积序列重复沉积,旋回下部为纹层状白云岩,发育鸟眼孔构造,旋回上部为浅灰色中—厚层状具有溶蚀孔洞的中晶白云岩,可见沥青呈浸染状分布,反映了潮间带局限暴露环境—潮上带暴露环境的演化序列。C3-2发育于洗象池组上部,表现为MF14在纵向上叠置沉积,此旋回

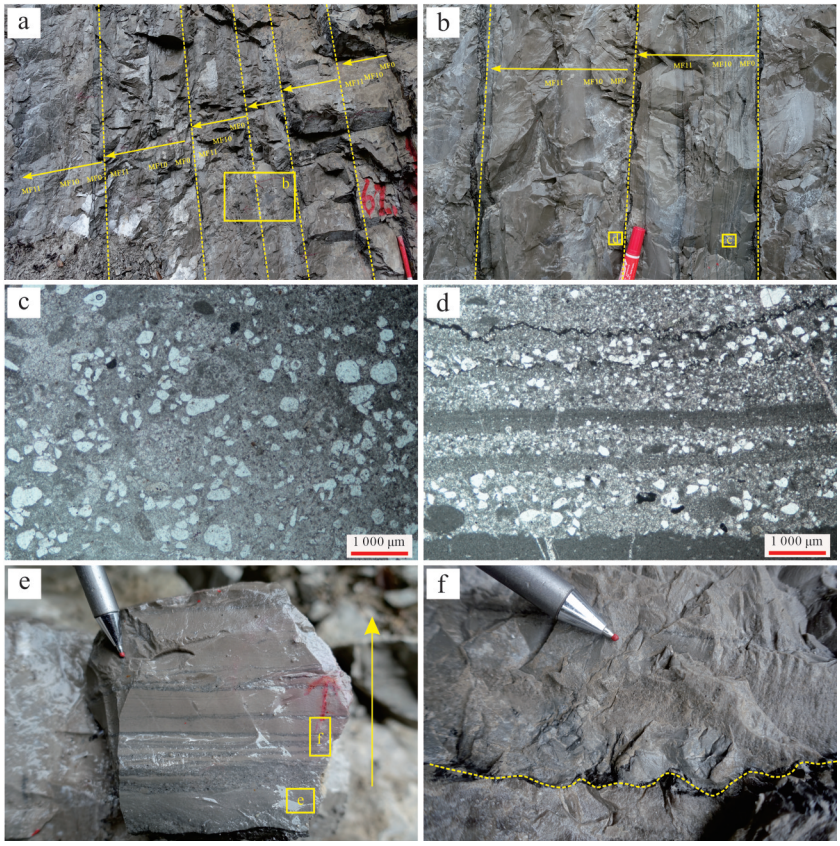

图6 川北城口修齐剖面上寒武统洗象池组潮下—潮间旋回C2-4宏—微观特征

(a)多个潮下—潮间沉积旋回;(b)沉积旋回局部照,每个旋回底部为厘米级暗色泥岩,发育底冲刷构造;旋回下部为砂质白云岩或细晶白云岩;旋回上部为砂质纹层状白云岩;(c)单个陆源碎屑正粒序旋回,下部砂质层厚且密集,上部砂质层薄且稀疏,自下而上,陆源碎屑粒度变细、含量变少;(d)凹凸不平底冲刷面,其下部含有大量砾屑和粗粒陆源碎屑,呈正粒序分布;(e)YMQ-62-1B,砂质白云岩,位于旋回底部;陆源石英分选差—中等,磨圆呈次棱角状—次圆状,总体呈细粒—中粒漂浮于粉晶白云石中,可见零星分布的砂屑颗粒及黄铁矿,单偏光;(f)YMQ-62-3B,纹层状白云岩位于旋回顶部,由泥晶白云岩(黑灰色)和砂质粉晶白云岩(浅色段)互层组成,所含陆源石英呈正粒序分布,整体粒度较旋回底部细,以粉砂为主,顶部发育缝合线,沥青充填,单偏光

Fig.6 Macro-micro characteristics of subtidal-intertidal cycle C2-4 from the upper Cambrian Xixiangchi Formation in the Xiuqi section, Chengkou, northern Sichuan Basin

(a) multiple subtidal-intertidal sedimentary cycles are developed, upper Cambrian Xixiangchi Formation, Xiuqi, Chengkou; (b) local illumination of sedimentary cycle, the bottom of each cycle is centimeter-level dark mudstone, and the bottom scour structure is developed, the lower part of the cycle is sandy dolomite or fine-grained dolomite, and the upper part of the cycle is sandy lamellar dolomite;(c) a single terrigenous clastic normal grain sequence cycle, the lower sandy layer is thick and dense, and the upper sandy layer is thin and sparse. From bottom to top, the grain size and content of terrigenous clastic become finer; (d) the lower part of the concave-convex uneven bottom scour surface contains a large amount of gravel and coarse-grained terrigenous debris, which is distributed in a positive order; (e) YMQ-62-1B, sandy dolomite, located at the bottom of the cycle; Terrestrial quartz is poorly sorted to medium, and rounded in sub-angular to sub-rounded shape. In general, fine-medium particles float in the powder crystal dolomite. Scattered distribution of sand particles and pyrite can be seen, PPL; (f) YMQ-62-3B, Lamellar dolomite is located at the top of the cycle; it is composed of mudstone dolomite (black-gray) and sandy silty dolomite (light-colored section). Terrestrial quartz is distributed in positive grain order. The overall grain size is finer than that at the bottom of the cycle, mainly silty sand, with sutures at the top and asphalt filling, PPL

主要发育浅灰色中—厚层状细晶、中晶白云岩,发育大量溶蚀孔、洞、缝,被白云石、方解石及有机质充填,部分层位可见沥青顺层、穿层浸染,岩溶作用明显。推测水体深度变浅,水体盐度增加,原有泥晶沉积物发生重结晶并出露地表,大气淡水对其进行淋滤改造形成溶蚀孔洞。反映潮上带蒸发、暴露环境。

城口地区晚寒武世洗象池组具有明显的风暴沉积特征,由于风暴作用强度及距离风暴中心远近不同,形成的风暴沉积序列不同。理想的浅水碳酸盐岩风暴沉积序列主要由5个沉积单元构成,由下至上分别为底冲刷面及砾屑段(A)、粒序段(B)、平行层理段(C)、丘状交错层理段(D)、风暴远端浊流沉积段(E)(Aigner, 1985)。通过对洗象池组沉积微相、沉积序列划分,共识别出三类主要风暴沉积序列:C1-3由底冲刷面及砾屑段(A)构成;C1-5由底冲刷面及砾屑段(A)、粒序段(B)构成;C2-2由底冲刷面及砾屑段(A)、粒序段(B)、丘状交错层理段(D)、风暴远端浊流沉积段(E)构成。

沉积序列随着相对海平面的升降而变化,岩性、厚度、沉积构造均揭示出这种特征,洗象池组沉积序列具有明显的向上变浅的沉积特征,为典型的碳酸盐岩台地向上变浅序列(图7)。潮下旋回发育于潮下带低能水体环境—潮下带振荡水体环境,主要发育于快速海侵时期,以薄层的泥质岩与风暴作用形成的颗粒岩沉积为主;海退时,伴随发育砂质沉积。潮下—潮间旋回主要发育于潮下带低能水体环境—潮下带振荡水体环境—潮间带局限暴露环境,其主要发育于缓慢海退时期,当相对海平面下降时,旋回下部泥质岩的厚度减少,旋回上部陆源碎屑—混积沉积增多,暴露成因的竹叶状砾屑以及沉积构造增多。潮间—潮上旋回发育于潮间带局限暴露环境—潮上带蒸发、暴露环境,主要发育于海退时期,随着相对海平面变浅,大气淡水溶蚀作用形成的孔缝增加,暴露程度不断升高。

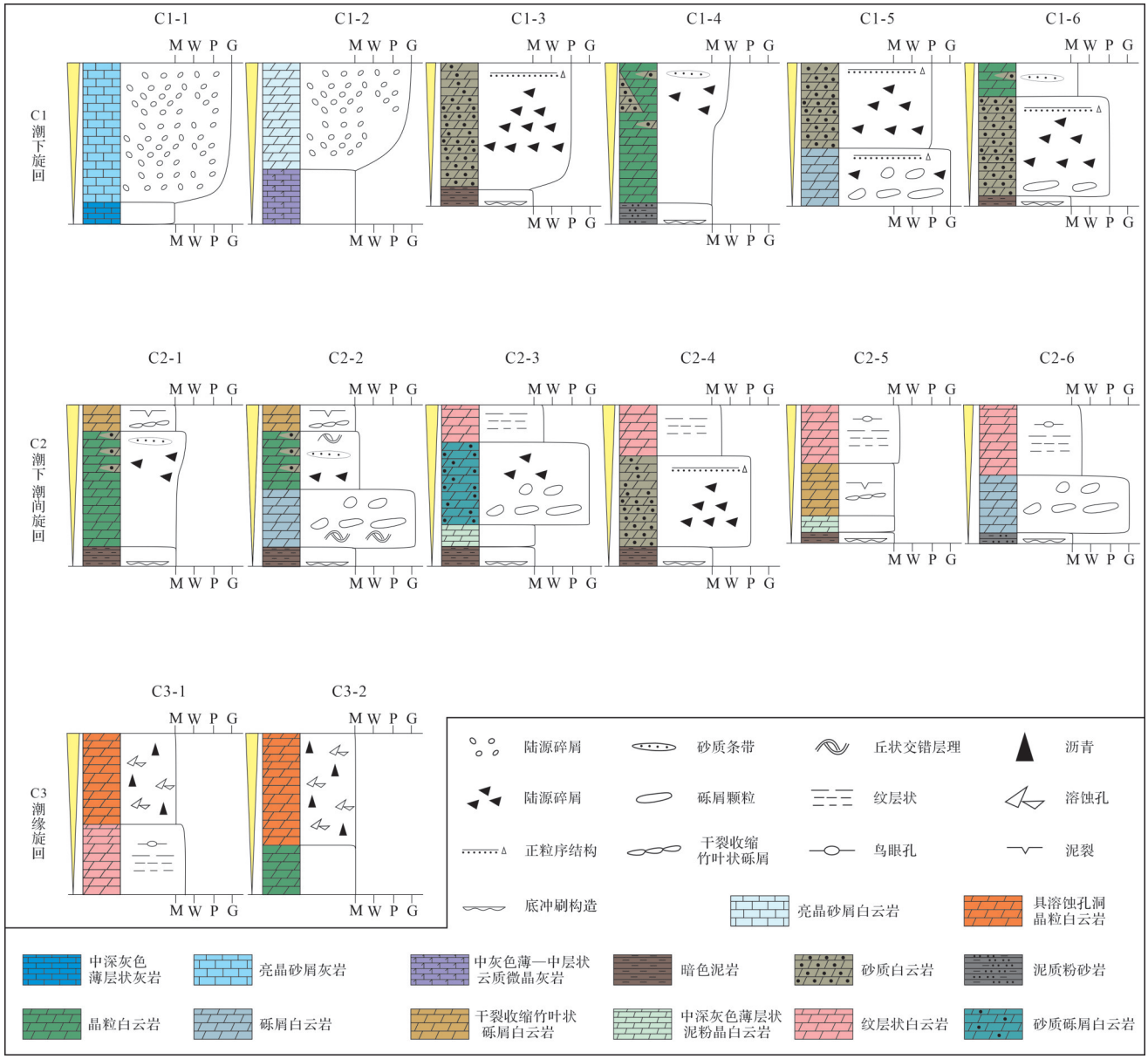

图7　川北城口修齐剖面上寒武统洗象池组典型沉积旋回示意图

M.泥晶结构;W.粒泥结构;P.泥粒结构;G.颗粒结构

Fig.7　Schematic diagram of typical sedimentary cycles of the upper Cambrian Xixiangchi Formation in the Xiuqi section, Chengkou, northern Sichuan Basin

M. mudstone structure; W. wackstone structure; P. packstone structure; G. grainstone structure

4 沉积环境演化及海平面变化

基于城口洗象池组剖面的野外沉积学特征解析,结合室内镜下薄片鉴定,识别了高精度向上变浅沉积序列,并判识了沉积环境。综合认为洗象池组沉积相类型以潮下带潟湖沉积与颗粒滩沉积、潮间带混积潮坪沉积、潮上带蒸发(岩溶)沉积为主。沉积物类型受潮汐、波浪、风暴等作用强烈控制,沉积环境演化受全球海平面波动、区域构造活动以及碳酸盐岩沉积速率综合影响。依据纵向演化的沉积微相、沉积旋回形成的沉积环境相对水深变化绘制相对海平面变化曲线,发现晚寒武世洗象池组相对海平面经历3次海侵—海退次级旋回,由下至上次级旋回下部深水沉积物厚度依次减少,而旋回上部浅水沉积以及暴露程度逐渐增加,反映洗象池组整体呈现海退趋势,详细沉积环境演化过程以及海平面变化历程如下所述(图8)。

次级旋回Ⅰ由洗象池组下段(26~56层)构成,厚度约为54 m。演化序列主要由C1-1、C1-2、C1-3、C1-4、C1-5、C2-1、C2-2沉积旋回在纵向上叠置沉积构成,总体表现为旋回下段主要由C1-1构成,旋回中段主要由C1-2、C1-3、C1-4、C1-5构成,旋回上段主要由C2-1、C2-2构成。演化序列为泥粉晶灰岩(海侵)、浅潮下带颗粒滩沉积(海侵)、深潮下带泥页岩沉积(最大海泛面)、浅潮下带颗粒滩沉积伴有风暴作用(海退)、潮间带竹叶状砾屑沉积(海退)。

次级旋回Ⅱ由洗象池组中段(57~85层)构成,厚度约为46 m。演化序列主要由C1-4、C1-5、C2-3、C2-4、C2-5、C2-6沉积旋回在纵向上重复沉积构成,总体表现为旋回下段主要由C1-4、C1-5、C2-3构成,旋回中段主要由C1-5、C2-4、C2-5构成,旋回上段主要由C2-5、C2-6构成。演化序列为深潮下带泥页岩与潟湖沉积(海侵)、浅潮下带颗粒滩沉积伴有风暴作用(海退)、潮间带纹层状白云岩与混积潮坪沉积(海退)。

次级旋回Ⅲ由洗象池组上段(86~117层)构成,厚度约为45 m。演化序列主要由C1-6、C2-6、C3-1、C3-2沉积旋回在纵向上重复沉积构成,总体表现为旋回下段主要由C1-6、C2-6构成,旋回中段主要由C2-5、C2-6构成。旋回上段主要由C3-1、C3-2构成,演化序列为深潮下带泥页岩沉积(海侵)、浅潮下带颗粒滩沉积(海退)、潮间带纹层状白云岩沉积与混积潮坪沉积(海退)、潮上带岩溶沉积伴有沥青浸染(海退),顶部发育古风化壳与不整合面。

5 沉积模式及其地质意义

通过识别晚寒武世洗象池组碳酸盐岩向上变浅序列并判识沉积环境,进一步明确了洗象池组沉积特征、沉积环境演化规律,并综合前人研究(黄福喜等,2011;井攀等,2016a;井攀,2017;张芮,2018),建立了上扬子北缘晚寒武世洗象池组浅水局限碳酸盐岩台地的沉积模式(图9)。该模式依据海平面变化以及波浪、潮汐作用影响的范围,将其沉积环境划分为潮下带、潮间局限环境(弱暴露)、潮上暴露环境。在深水潮下带低能环境中,主要发育泥页岩,泥质粉砂岩、泥粉晶灰岩与云质微晶灰岩,在该环境中,水动力较弱,几乎不含颗粒结构;在浅水潮下带振荡环境中,主要发育颗粒滩沉积,最主要为砂屑滩沉积;在潮间带局限环境中,主要发育纹层状白云岩与干裂收缩竹叶状砾屑白云岩;在潮上暴露环境中,发育纹层状白云岩与具有溶蚀孔洞的晶粒白云岩,沥青呈浸染状分布。

综上所述,四川盆地晚寒武世洗象池组纵向上发育3个次级海侵—海退旋回,沉积环境受海平面变化影响,受潮汐、波浪以及风暴等作用的强烈控制,主要发育以云质潟湖亚相、台内颗粒滩亚相以及混积潮坪亚相为典型沉积特征的局限碳酸盐岩台地沉积。次级旋回Ⅰ主要发育由潮下带沉积微相构成的沉积旋回,次级旋回Ⅱ主要发育由潮下—潮间带沉积微相构成的沉积旋回,次级旋回Ⅲ主要发育由潮间—潮上沉积微相构成的沉积旋回。由下至上,各个次级旋回下部潮下带沉积微相厚度依次减少,而次级旋回上部潮间—潮上带沉积微相厚度以及暴露程度逐渐增加。由下至上,沉积微相和沉积旋回在纵向的变化均指示由深水沉积环境不断向浅水暴露沉积环境演化,反映洗象池组海平面整体呈海退趋势。同时,其顶部发育古风化壳,也进一步表明该地区晚寒武世发生较大程度的海退侵蚀事件。在年代地层和晚寒武世层序地层研究基础上,通过对比年代地层和演化特征,发现扬子地台洗象池组顶部发育区域性不整合面(黄福喜等,2011)。华北地台晚寒武世末期发育暴露间断面(梅冥相和马永生,2003),塔里木地台晚寒武世顶部的局限沉积(朱金富等,2008;黄渊等,2022)均揭示晚寒武世海平面呈

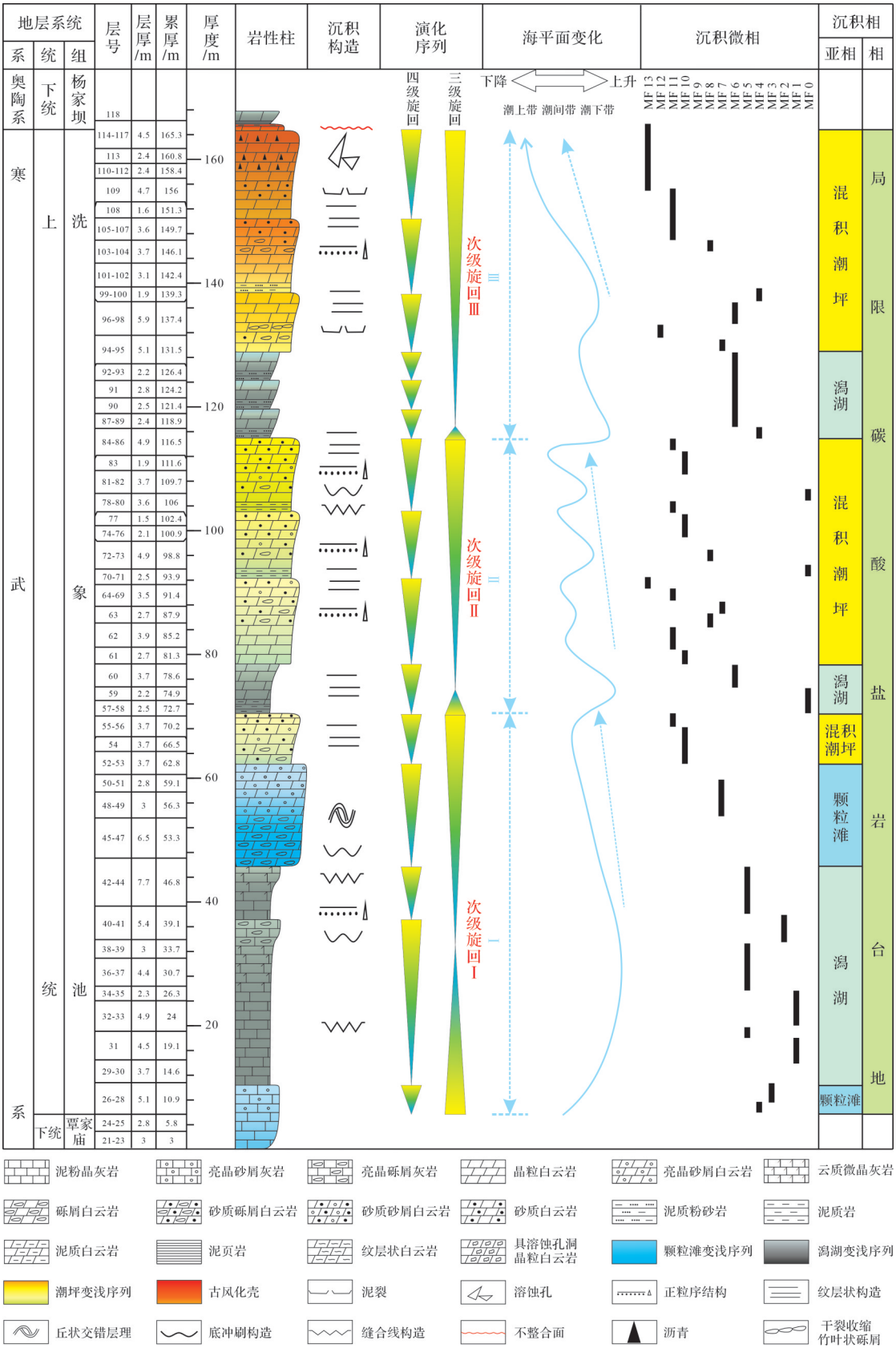

图8　川北城口修齐剖面上寒武统洗象池组沉积演化综合地层柱状图

Fig.8　Comprehensive stratigraphic histogram of the sedimentary evolution of the upper Cambrian Xixiangchi Formation in the Xiuqi section of Chengkou, northern Sichuan Basin

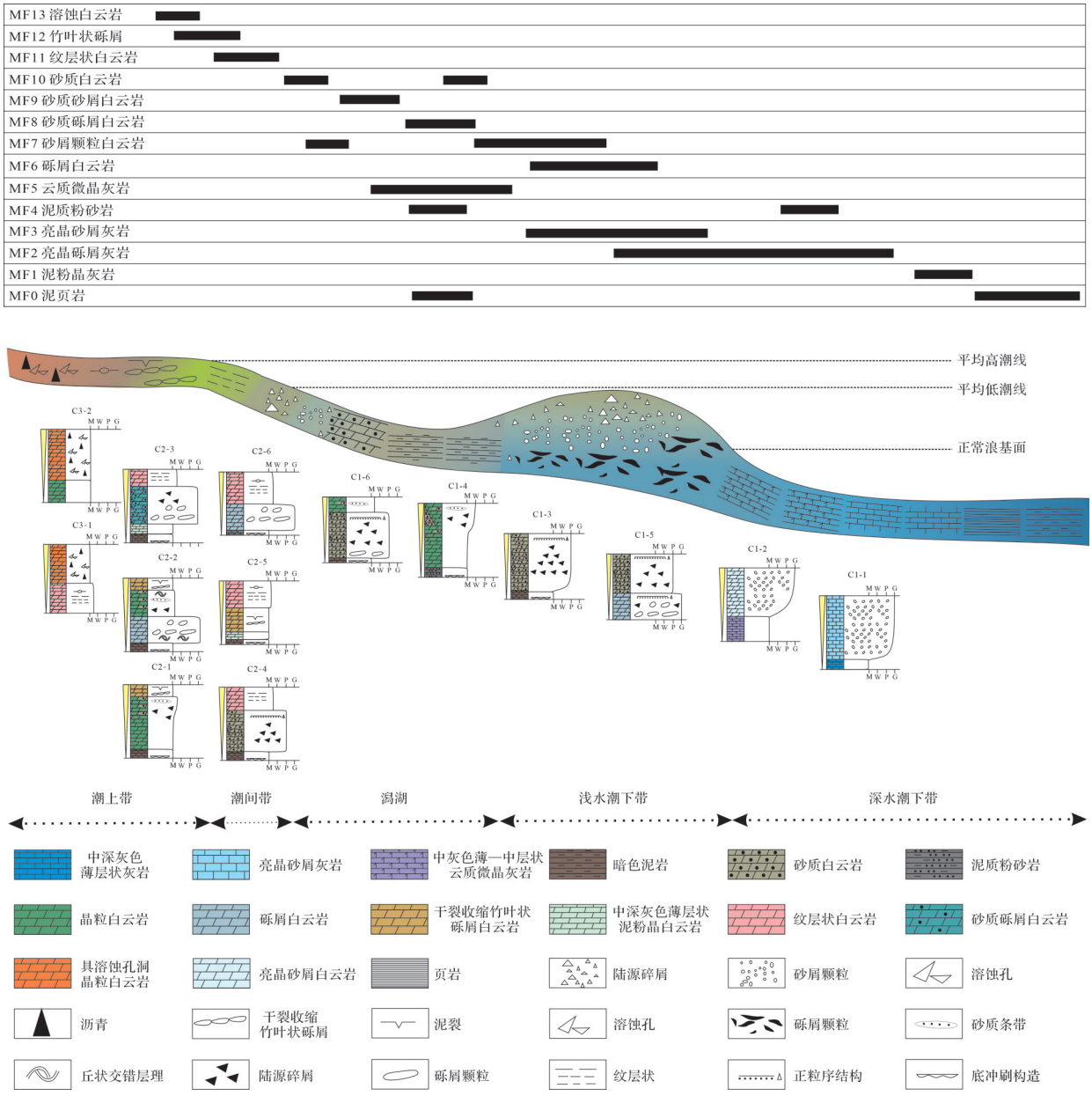

图9 川北城口修齐剖面上寒武统洗象池组沉积模式图

M.泥晶结构;W.粒泥结构;P.泥粒结构;G.颗粒结构

Fig.9 Sedimentary model of the upper Cambrian Xixiangchi Formation in the Xiuqi section of Chengkou, northern Sichuan Basin

M. mudstone structure; W. wackstone structure; P. packstone structure; G. grainstone structure

海退趋势,与美国晚寒武世牙形类*C.proavus*带底、*Fryxel-lodontus inornatus*亚带底的升降事件(Miller,1995)和澳大利亚晚寒武世的海退事件(Nicoll *et al.*,1992)研究结果一致,进一步证实了晚寒武世末期发生全球性海平面下降事件(张俊明等,2000)。

6 结论

(1) 根据不同岩石类型的组构差异以及碳酸盐岩微相分类原则,在洗象池组识别出14类沉积微相,其中常见的微相类型包括:MF0泥页岩、MF1泥粉晶灰岩、MF2亮晶砾屑灰岩、MF3亮晶砂屑灰岩、MF4泥质粉砂岩、MF5云质微晶灰岩、MF6砾屑白云岩、MF7亮晶砂屑白云岩、MF8砂质砾屑白云岩、MF9砂质砂屑白云岩、MF10砂质白云岩、MF11纹层状白云岩、MF12竹叶状砾屑白云岩、MF13具有溶蚀孔洞晶粒白云岩。

(2) 基于微相解释和纵向组合关系,识别出3种大类,共14种亚类向上变浅沉积序列(包含3类风暴

沉积序列)。旋回类型Ⅰ(C1):潮下沉积旋回(颗粒滩序列),发育6种亚类;旋回类型Ⅱ(C2):潮下—潮间沉积旋回(潟湖序列),发育6种亚类;旋回类型Ⅲ(C3):潮间—潮上沉积旋回(混积潮坪序列),发育2种亚类。

(3)利用高精度向上变浅序列判识沉积环境并揭示其演化过程。将洗象池组划分为三个次级海侵—海退旋回。次级旋回Ⅰ由洗象池组下段构成、次级旋回Ⅱ由洗象池组中段构成、次级旋回Ⅲ由洗象池组上段构成。其中,次级旋回Ⅰ主要发育潮下沉积旋回、潮下—潮间沉积旋回,次级旋回Ⅱ主要发育潮下沉积旋回、潮下—潮间沉积旋回,次级旋回Ⅲ主要发育潮下—潮间沉积旋回和潮间—潮上沉积旋回。洗象池组由下至上整体表现为一个快速海侵—缓慢海退沉积序列,其顶部发育古风化壳与不整合面。

(4)四川盆地晚寒武世洗象池组沉积环境受相对海平面变化影响明显,受潮汐、波浪以及风暴作用强烈控制,是以浅潮下带颗粒滩亚相、潮下带潟湖亚相以及混积潮坪亚相为典型沉积特征的局限碳酸盐岩台地沉积。此外,晚寒武世洗象池组整体为一个海侵—海退旋回,在其顶部发育区域性分布的暴露不整合面,进一步证实了晚寒武世末期发生全球海平面下降事件。

参考文献(References)

白壮壮,杨威,谢武仁,等. 2021. 川中地区寒武系洗象池群层序地层及台内滩发育特征[J]. 天然气地球科学,32(2):191-204. [Bai Zhuangzhuang, Yang Wei, Xie Wuren, et al. 2021. Sequence stratigraphy of Cambrian Xixiangchi Group and development characteristics of intra-platform bank in central Sichuan Basin[J]. Natural Gas Geoscience, 32(2): 191-204.]

曹庆超,白壮壮,李浩武,等. 2021. 测井数据小波变换在川中寒武系洗象池群层序地层划分中的应用[J]. 地质科技通报,40(4):242-251. [Cao Qingchao, Bai Zhuangzhuang, Li Haowu, et al. 2021. Application of wavelet transformation of logging data in sequence stratigraphic division of Cambrian Xixiangchi Group in central Sichuan Basin[J]. Bulletin of Geological Science and Technology, 40 (4): 242-251.]

陈洪德,田景春,刘文均,等. 2002. 中国南方海相震旦系—中三叠统层序划分与对比[J]. 成都理工学院学报,29(4):355-379. [Chen Hongde, Tian Jingchun, Liu Wenjun, et al. 2002. Division and correlation of the sequences of marine Sinian system to Middle Triassic series in the south of China[J]. Journal of Chengdu University of Technology, 29(4): 355-379.]

陈文,刘鑫,曾乙洋. 2016. 川中地区洗象池组小层划分及沉积演化特征[J]. 天然气勘探与开发,9(1):6-8,16. [Chen Wen, Liu Xin, Zeng Yiyang. 2016. Substrata division and sedimentary evolution of Xixiangchi Formation, central Sichuan Basin[J]. Natural Gas Exploration and Development, 39(1): 6-8, 16.]

邓成昆,黎霆,杨伟强,等. 2022. 川中地区中上寒武统洗象池组颗粒滩储集层特征及主控因素[J]. 古地理学报,24(2):292-307. [Deng Chengkun, Li Ting, Yang Weiqiang, et al. 2022. Characteristics and main controlling factors of shoal reservoirs in the middle-upper Cambrian Xixiangchi Formation, central Sichuan Basin[J]. Journal of Palaeogeography, 24(2): 292-307.]

Flügel E. 2006. 碳酸盐岩微相:分析、解释及应用[M]. 马永生,译. 北京:地质出版社:718-723. [Flügel E. 2006. Microfacies of carbonate rocks: Analysis, interpretation and application[M]. Ma Yongsheng, trans. Beijing: Geological Publishing House: 718-723.]

谷明峰,李文正,邹倩,等. 2020. 四川盆地寒武系洗象池组岩相古地理及储层特征[J]. 海相油气地质,25(2):162-170. [Gu Mingfeng, Li Wenzheng, Zou Qian, et al. 2020. Lithofacies palaeogeography and reservoir characteristics of the Cambrian Xixiangchi Formation in Sichuan Basin[J]. Marine Origin Petroleum Geology, 25(2): 162-170.]

郭艳波,任冠雄,叶朝阳,等. 2021. 四川盆地东部寒武系洗象池组白云岩成因研究[J]. 河南科技,40(34):150-152. [Guo Yanbo, Ren Guanxiong, Ye Chaoyang, et al. 2021. Research on the genesis of dolomites in the Cambrian Xixiangchi Formation in the eastern Sichuan Basin[J]. Henan Science and Technology, 40(34): 150-152.]

胡朝阳. 2015. 龙女寺—广安地区寒武系洗象池组储层特征及有利区预测[D]. 成都:西南石油大学:1-78. [Hu Chaoyang. 2015. Reservoir characteristics and favorable area prediction of the Cambrian Xixiangchi Formation in the Longnvsi-Guang'an area[D]. Chengdu: Southwest Petroleum University: 1-78.]

黄丹. 2012. 四川盆地西部上二叠统长兴组—下三叠统飞仙关组层序地层学研究[D]. 荆州:长江大学:1-75. [Huang Dan. 2012. Research on sequence stratigraphy of the upper permianseries Changxing Formation and the Lower Triassic Feixianguan Formation in western Sichuan Basin[D]. Jingzhou: Yangtze University: 1-75.]

黄福喜,陈洪德,侯明才,等. 2011. 中上扬子克拉通加里东期(寒武—志留纪)沉积层序充填过程与演化模式[J]. 岩石学报,27(8):2299-2317. [Huang Fuxi, Chen Hongde, Hou Mingcai, et al. 2011. Filling process and evolutionary model of sedimentary sequence of Middle-Upper Yangtze Craton in Caledonian(Cambrian-Silurian)[J]. Acta Petrologica Sinica, 27(8): 2299-2317.]

黄渊,段太忠,樊太亮,等. 2022. 塔河地区寒武纪碳酸盐岩台地沉积演化史与成因机制:来自地层沉积正演模拟的启示[J]. 石油学报,43(5):617-636. [Huang Yuan, Duan Taizhong, Fan Tailiang, et al. 2022. Depositional evolution history and formation mechanism of Cambrian carbonate platforms in Tahe area: Insights from stratigraphic forward modelling[J]. Acta Petrolei Sinica, 43(5): 617-636.]

贾鹏,李伟,卢远征,等. 2016. 四川盆地中南部地区洗象池群沉积旋回的碳氧同位素特征及地质意义[J]. 现代地质,30(6):1329-1338. [Jia Peng, Li Wei, Lu Yuanzheng, et al. 2016. Carbon and oxygen isotopic compositions and their evolution records of the Xixiangchi Group in sedimentary sequences of central-southern Sichuan Basin and their geological implications[J]. Geoscience, 30(6): 1329-1338.]

金鑫,宋金民,刘树根,等. 2021. 四川盆地周缘灯影组风暴沉积特征及其地质意义[J]. 天然气工业,41(10):39-49. [Jin Xin, Song Jinmin, Liu Shugen, et al. 2021. Characteristics and geological implications of Dengying Formation tempestites in the periphery of the Sichuan Basin[J]. Natural Gas Industry, 41(10): 39-49.]

井攀. 2017. 川中南部地区寒武系洗象池组层序地层及沉积相研究[D]. 成都:成都理工大学:1-84. [Jing Pan. 2017. The research on the sequence and the distribution of sedimentary facies of upper Cambrian Xixiangchi Formation in the southern aera of central Sichuan Basin[D]. Chengdu: Chengdu University of Technology: 1-84.]

井攀,黄加力,百成钢,等. 2016a. 四川盆地洗象池组层序地层及沉积相研究现状[J]. 山东化工,45(11):65-66, 69. [Jing Pan, Huang Jiali, Bai Chenggang, et al. 2016. The present research situation of sequence and sedimentary facies of Xixiangchi Formation of Sichuan Basin[J]. Shandong Chemical Industry, 45(11): 65-66, 69.]

井攀,徐芳艮,肖尧,等. 2016b. 川中南部地区上寒武统洗象池组沉积相及优质储层台内滩分布特征[J]. 东北石油大学学报,40(1):40-50. [Jing Pan, Xu Fanggen, Xiao Yao, et al. 2016. The bank facies distribution of upper Cambrian Xixiangchi Formation in the southern area of central Sichuan Basin[J]. Journal of Northeast Petroleum University, 40(1): 40-50.]

李璐萍,梁金同,刘四兵,等. 2022. 川中地区寒武系洗象池组白云岩储层成岩作用及孔隙演化[J]. 岩性油气藏,34(3):39-48. [Li Luping, Liang Jintong, Liu Sibing, et al. 2022. Diagenesis and pore evolution of dolomite reservoirs of Cambrian Xixiangchi Formation in central Sichuan Basin[J]. Lithologic Reservoirs, 34(3): 39-48.]

李伟,樊茹,贾鹏,等. 2019. 四川盆地及周缘地区中上寒武统洗象池群层序地层与岩相古地理演化特征[J]. 石油勘探与开发,46(2):226-240. [Li Wei, Fan Ru, Jia Peng, et al. 2019. Sequence stratigraphy and lithofacies paleogeography of middle–upper Cambrian Xixiangchi Group in Sichuan Basin and its adjacent area, SW China [J]. Petroleum Exploration and Development, 46(2): 226-240.]

李伟,余华琪,邓鸿斌. 2012. 四川盆地中南部寒武系地层划分对比与沉积演化特征[J]. 石油勘探与开发,39(6):681-690. [Li Wei, Yu Huaqi, Deng Hongbin. 2012. Stratigraphic division and correlation and sedimentary characteristics of the Cambrian in central-southern Sichuan Basin[J]. Petroleum Exploration and Development, 39(6): 681-690.]

李文正,张建勇,郝毅,等. 2019. 川东南地区洗象池组碳氧同位素特征、古海洋环境及其与储集层的关系[J]. 地质学报,93(2):487-500. [Li Wenzheng, Zhang Jianyong, Hao Yi, et al. 2019. Characteristics of carbon and oxygen isotopic, paleoceanographic environment and their relationship with reservoirs of the Xixiangchi Formation, southeastern Sichuan Basin[J]. Acta Geologica Sinica, 93(2): 487-500.]

李茜,朱光有,李婷婷,等. 2022. 川中地区寒武系洗象池组白云岩Mg同位素特征与成因机制[J]. 石油学报,43(11):1585-1603. [Li Xi, Zhu Guangyou, Li Tingting, et al. 2022. Mg isotopic characteristics and genetic mechanism of dolomite of Cambrian Xixiangchi Formation in central Sichuan Basin[J]. Acta Petrolei Sinica, 43(11): 1585-1603.]

罗志立. 2012. 峨眉地裂运动观对川东北大气区发现的指引作用[J]. 新疆石油地质,33(4):401-407. [Luo Zhili. 2012. Guidance function of Emei Taphrogenesis viewpoint on discovery of large gas province in northeastern Sichuan[J]. Xinjiang Petroleum Geology, 33(4): 401-407.]

梁乘鹏. 2019. 四川盆地寒武系洗象池组层序岩相古地理研究[D]. 成都:成都理工大学:1-69. [Liang Chengpeng. 2019. Study on sequence lithofacies paleogeography of Xixiangchi Formation of Cambrian in Sichuan Basin[D]. Chengdu: Chengdu University of Technology: 1-69.]

林怡,陈聪,山述娇,等. 2017. 四川盆地寒武系洗象池组储层基本特征及主控因素研究[J]. 石油实验地质,39(5):610-617. [Lin Yi, Chen Cong, Shan Shujiao, et al. 2017. Reservoir characteristics and main controlling factors of the Cambrian Xixiangchi Formation in the Sichuan Basin[J]. Petroleum Geology & Experiment, 39(5): 610-617.]

刘鑫,曾乙洋,文龙,等. 2018. 川中地区洗象池组有利沉积相带分布预测[J]. 天然气勘探与开发,41(2):15-21. [Liu Xin, Zeng Yiyang, Wen Long, et al. 2018. Distribution prediction on favorable sedimentary-facies belts of Xixiangchi Formation, central Sichuan Basin[J]. Natural Gas Exploration and Development, 41(2): 15-21.]

梅冥相,马永生. 2003. 华北地台晚寒武世层序地层及其与北美地台海平面变化的对比[J]. 沉积与特提斯地质,23(4):14-26. [Mei Mingxiang, Ma Yongsheng. 2003. Sequence stratigraphy of the late Cambrian strata on the North China Platform and the correlation of the sea-level changes with the North America Platform[J]. Sedimentary Geology and Tethyan Geology, 23(4): 14-26.]

潘安. 2019. 大巴山中西段地质景观分类与成因研究[D]. 成都:成都理工大学:1-149. [Pan An. 2019. Research on geological landscape classification and genesis of mid-western section of Daba Mountains[D]. Chengdu: Chengdu University of Technology: 1-149.]

齐哲,侯明才,王瀚,等. 2022. 上扬子西北缘晚震旦世古环境演化[J]. 地质学报,96(7):2281-2294. [Qi Zhe, Hou Mingcai, Wang Han, et al. 2022. Paleo-environmental evolution of Late Sinian Period in the northwestern margin of Upper Yangtze[J]. Acta Geologica Sinica, 96(7): 2281-2294.]

石书缘,胡素云,洪海涛,等. 2015. 四川盆地寒武系洗象池组白云岩

储层特征及油气勘探前景[C]//中国地质学会沉积地质专业委员会，中国矿物岩石地球化学学会沉积学专业委员会．2015年全国沉积学大会沉积学与非常规资源论文摘要集．武汉：189-190. [Shi Shuyuan, Hu Suyun, Hong Haitao, et al. 2015. Dolomite reservoir characteristics and oil and gas exploration prospects of Cambrian Xixiangchi Formation in Sichuan Basin[C]//Sedimentary Geology Professional Committee of Geological Society of China, Sedimentology Professional Committee of Chinese Society of Mineralogy, Petrology and Geochemistry. Sedimentology and unconventional resource abstracts of the 2015 national congress of sedimentology. Wuhan: 189-190.]

谭秀成，李凌，刘宏，等．2014．四川盆地中三叠统雷口坡组碳酸盐台地巨型浅滩化研究[J]．中国科学：地球科学，2014，44(3)：457-471. [Tan Xiucheng, Li Ling, Liu Hong, et al. 2014. Mega-shoaling in carbonate platform of the Middle Triassic Leikoupo Formation, Sichuan Basin, Southwest China[J]. Science China Earth Sciences, 44(3): 457-471.]

Tucker M E, Wright V P. 2015. 碳酸盐岩沉积学[M]. 沈安江，王小芳，郑剑锋，等译．北京：石油工业出版社：52-61. [Tucker M E, Wright V P. 2015. Carbonate sedimentology[M]. Shen Anjiang, Wang Xiaofang, Zheng Jianfeng, et al. , trans. Beijing: Petroleum Industry Press: 52-61.]

王瀚，李智武，刘树根，等．2019．扬子地台北缘城口地区上寒武统洗象池组风暴沉积特征及其地质意义[J]．石油实验地质，41(2)：176-184. [Wang Han, Li Zhiwu, Liu Shugen, et al. 2019. Sedimentary characteristics and geological significance of tempestites in the upper Cambrian Xixiangchi Formation, Chengkou area, northern margin of the Yangtze Platform[J]. Petroleum Geology & Experiment, 41(2): 176-184.]

王牧源，牟传龙，王秀平，等．2024．川北旺苍地区奥陶系沉积特征与风暴沉积的发现[J]．沉积与特提斯地质，44(2)：311-325. [Wang Muyuan, Mou Chuanlong, Wang Xiuping, et al. 2024. Characteristics of Ordovician sedimentation and the discovery of storm deposition in the Wangcang area, northern Sichuan[J]. Sedimentary Geology and Tethyan Geology, 44(2): 311-325.]

文华国，梁金同，周刚，等．2022．四川盆地及周缘寒武系洗象池组层序—岩相古地理演化与天然气有利勘探区带[J]．岩性油气藏，34(2)：1-16. [Wen Huaguo, Liang Jintong, Zhou Gang, et al. 2022. Sequence-based lithofacies paleogeography and favorable natural gas exploration areas of Cambrian Xixiangchi Formation in Sichuan Basin and its periphery[J]. Lithologic Reservoirs, 34(2): 1-16.]

夏康杰．2020．川北寒武系洗象池群储层特征研究[D]．成都：成都理工大学：1-67. [Xia Kangjie. 2020. Studies on reservoir characteristics of the Cambrian Xixiangchi Group in northern Sichuan Basin [D]. Chengdu: Chengdu University of Technology: 1-67.]

谢环羽，姜在兴，王培玺，等．2021．中—上扬子地区寒武系层序地层格架[J]．石油学报，42(7)：865-884. [Xie Huanyu, Jiang Zaixing, Wang Peixi, et al. 2021. Cambrian sequence stratigraphic framework in the Middle-Upper Yangtze area[J]. Acta Petrolei Sinica, 42(7): 865-884.]

张俊明，王海峰，李国祥．2000．华北与扬子地台晚寒武世末期至早奥陶世早期层序地层对比及海平面升降事件[J]．地层学杂志，24(增刊)：359-369. [Zhang Junming, Wang Haifeng, Li Guoxiang. 2000. Sequence stratigraphic correlation and eustatic events from latest Cambrian to early Early Ordovician between North China and Yangtze Platforms[J]. Journal of Stratigraphy, 24(Suppl.): 359-369.]

张满郎，谢增业，李熙喆，等．2010．四川盆地寒武纪岩相古地理特征[J]．沉积学报，28(1)：128-139. [Zhang Manlang, Xie Zengye, Li Xizhe, et al. 2010. Characteristics of lithofacies paleogeography of Cambrian in Sichuan Basin[J]. Acta Sedimentologica Sinica, 28 (1): 128-139.]

张芮．2018．川北九龙山及周缘地区寒武系沉积相及与生储盖的关系[D]．成都：西南石油大学：1-69. [Zhang Rui. 2018. Cambrian sedimentary facies and their relationship with source, reservoir, and cap rocks in the Jiulong Mountains and surrounding areas of northern Sichuan[D]. Chengdu: Southwest Petroleum University: 1-69.]

章学刚，熊冉，邓庆杰，等．2022．四川盆地洗象池组颗粒滩沉积组合特征及沉积控储机理[J]．科学技术与工程，22(4)：1389-1398. [Zhang Xuegang, Xiong Ran, Deng Qingjie, et al. 2022. Sedimentary characteristics and controls of reservoirs of the shoals of Xixiangchi Formation in Sichuan Basin[J]. Science Technology and Engineering, 22(4): 1389-1398.]

朱金富，于炳松，黄文辉，等．2008．塔里木盆地塔中地区晚寒武世—奥陶世碳酸盐岩碳、氧同位素特征[J]．大庆石油地质与开发，27(1)：39-42. [Zhu Jinfu, Yu Bingsong, Huang Wenhui, et al. 2008. Carbon and oxygen isotope features of late Cambrian-Ordovician in central Tarim Basin[J]. Petroleum Geology & Oilfield Development in Daqing, 27(1): 39-42.]

Aigner T. 1985. Storm depositional systems[M]. Berlin: Springer-Verlag.

Coogan A H. 1969. Recent and ancient carbonate cyclic sequences[M]// Elam J G, Chuber S. Cyclic sedimentation in the Permian basin. Midland, Texas: West Texas Geological Society: 5-27.

Fischer A G. 1964. The Lofer cyclothems of the alpine Triassic[J]. Bulletin Geological Survey Kansas, 169: 107-149.

Flügel E. 2010. Microfacies of carbonate rocks: Analysis, interpretation and application[M]. Berlin: Springer: 587-590.

Goldhammer R K, Dunn P A, Hardie L A. 1987. High frequency glacio-eustatic sealevel oscillations with Milankovitch characteristics recorded in Middle Triassic platform carbonates in northern Italy[J]. American Journal of Science, 287(9): 853-892.

Goldhammer R K, Dunn P A, Hardie L A. 1990. Depositional cycles, composite sea-level changes, cycle stacking patterns, and the hierarchy of stratigraphic forcing: Examples from Alpine Triassic platform carbonates[J]. GSA Bulletin, 102(5): 535-562.

Imbrie J, Imbrie J Z. 1980. Modeling the climatic response to orbital variations[J]. Science, 207(4434): 943-953.

James N P. 1978. Facies models 10. Reefs[J]. Geoscience Canada, 5

(1): 16-26.

Laporte L F. 1967. Carbonate deposition near mean sea-level and resultant facies mosaic: Manlius Formation (Lower Devonian) of New York State[J]. AAPG Bulletin, 51(1): 73-101.

Miller J F. 1995. Acid insoluble residues, regressive-transgressive events, and conodont biostratigraphy in the upper Cambrian and Lower Ordovician of western Utah and Central Texas[C]//7th international symposium on the Ordovician system. Las Vegas: Society for Sedimentary Geology: 99-104.

Nicoll R S, Laurie J R, Shergold J H, et al. 1992. Preliminary correlation of latest Cambrian to Early Ordovician sea-level events in Australia and Scandinavia[M]//Webby B D, Laurie J R. Global perspectives on Ordovician geology. Rotterdam: A. A. Balkema: 381-394.

Wang H, Liu S G, Hou M C, et al. 2022. Petrological and micrometer-scale geochemical constraints on chert origins in the Dengying Formation, Yangtze Block, South China: Implications for Late Ediacaran hydrothermal activity and tectonic setting[J]. Precambrian Research, 370: 106531.

Wilson J L. 1975. Grainstones and types of carbonate shelf cycles (Abstract)[J]. Houston Geological Society Bulletin, 18(4): 2.

Recognition and Depositional Environment Interpretation of the Shallowing-Upward Sequence: A case study from the Cambrian Xixiangchi Formation in the northern margin of the Upper Yangtze

TANG JiaQuan[1], WANG Han[1], ZHANG YaoYun[2], WANG Bin[1], DENG HaoShuang[1], HOU MingCai[1]

1. State Key Laboratory of Oil & Gas Reservoir Geology and Exploration (Chengdu University of Technology), Chengdu 610059, China

2. Southwest Geophysical Exploration Research Institute of China Petroleum Group Eastern Geophysical Exploration Co., Ltd, Chengdu 610093, China

Abstract: [**Objective**] Upward shallowing sequences are widely developed in shallow-water carbonate environments, and the identification of upward shallowing sequences in deep-water carbonate rocks has a unique advantage in analyzing the evolutionary process of shallow-water carbonate sedimentary environments. Analyzing the high-precision upward shallowing sequences of the late Cambrian Xixiangchi Formation in the Upper Yangtze region can provide important references for understanding the late Cambrian global environmental changes.[**Methods**] Detailed field sedimentological dissection and indoor microfacies analysis were conducted on the upper Cambrian Xixiangchi Formation in Chengkou town along the northern margin of the Upper Yangtze. Carbonate rock decimeter- and meter-scale upward shallowing sequences were identified, and their compositional characteristics and vertical superposition relationships were analyzed to explore the sedimentary environment and its evolution in the late Cambrian of the Upper Yangtze region.[**Results**] Based on detailed field observations and thin section identification, and referring to the Flügel sedimentary microfacies classification scheme, 14 microfacies types were identified in the Xixiangchi Formation at the Chengkou section, including subtidal sedimentary microfacies MF0-MF10; intertidal sedimentary microfacies MF11-MF12; and supratidal sedimentary microfacies MF13. These microfacies include: MF0 argillaceous shale, MF1 micrite, MF2 bright crystal gravel limestone, MF3 bright crystal sand limestone, MF4 muddy siltstone, MF5 dolomitic microcrystalline limestone, MF6 gravel dolomite, MF7 bright crystal sand dolomite, MF8 sandy gravel dolomite, MF9 sandy dolarenite, MF10 sandy dolomite, MF11 laminated dolomite, MF12 bamboo leaf-like gravel dolomite, and MF13 grain dolomite with dissolution pores. Based on microfacies interpretation and

Foundation: National Natural Science Foundation of China, No. 42102138; Open Fund of Key Laboratory of Deep-time Geography and Environment Reconstruction and Applications of Ministry of Natural Resources, Chengdu University of Technology, No. DGERA 20221103

Corresponding author: HOU MingCai, E-mail: houmc@cdut.edu.cn

vertical stacking relationships, C1-1 to C1-6 decimeter-scale upward shallowing subtidal, C2-1 to C2-6 decimeter-scale upward shallowing subtidal to intertidal, and C3-1 to C3-2 decimeter-scale upward shallowing intertidal to supratidal sedimentary sequences were identified. These decimeter-scale upward shallowing cycles constitute three secondary transgressive-regressive sedimentary cycles, which from bottom to top, constitute the rapid transgression-slow regression upward shallowing sedimentary cycle of the Xixiangchi Formation. Secondary cycle I was developed by subtidal sedimentary microfacies, secondary cycle II was developed by subtidal to intertidal sedimentary microfacies, and secondary cycle III was developed by intertidal to supratidal sedimentary microfacies. From bottom to top, the thickness of subtidal sedimentary microfacies in the lower part of each secondary cycle decreases successively, whereas the thickness and exposure degree of intertidal to supratidal sedimentary microfacies in the upper part of each secondary cycle gradually increase.[**Conclusions**] Based on the identification of upward shallowing sedimentary sequences and the analysis of their compositional characteristics and vertical stacking relationships, the Xixiangchi Formation in the late Cambrian was significantly influenced by high-frequency sea level changes, strongly controlled by tides, waves, and storms. It experienced early rapid transgression and late slow regression, and underwent multiple secondary transgressive-regressive cycles, forming a limited carbonate platform sedimentation model characterized by mixed tidal flat subfacies, micritic lagoon subfacies, and intraplatform grain shoal subfacies. Furthermore, the development of paleo-weathering crust at the top indicates significant regression and erosion events in the late Cambrian in this region. By comparing with chronostratigraphic and evolutionary characteristics of platforms in the Yangtze Platform, North China Platform, Tarim Platform, United States, and Australia, it further confirms the global sea level fall events in the late Cambrian.

Key words: northern margin of Upper Yangtze Block; Xixiangchi Formation; microfacies of carbonate rocks; shallowing-upward sequence; sedimentary environment interpretation